Ultrasound in Med. & Biol., Vol. 35, No. 10, pp. 1737–1747, 2009

0301-5629/09/$–see front matter

ELSEVIER

doi:10.1016/j.ultrasmedbio.2009.05.002

● *Original Contribution*

FOCUSED ULTRASOUND EFFECTS ON NERVE ACTION POTENTIAL *IN VITRO*

VINCENT COLUCCI,* GARY STRICHARTZ,† FERENC JOLESZ,* NATALIA VYKHODTSEVA,* and KULLERVO HYNYNEN*‡

*Department of Radiology, Harvard Medical School and Brigham and Women's Hospital, Boston, MA, USA; †Department of Anesthesia, Harvard Medical School and Brigham and Women's Hospital, Boston, MA, USA; and ‡Sunnybrook Health Sciences Centre, Imaging Research, and Department of Medical Biophysics, University of Toronto, Toronto, ON, Canada

(*Received* 30 *January* 2009; *revised* 1 *May* 2009; *in final form* 4 *May* 2009)

Abstract—Minimally invasive applications of thermal and mechanical energy to selective areas of the human anatomy have led to significant advances in treatment of and recovery from typical surgical interventions. Image-guided focused ultrasound allows energy to be deposited deep into the tissue, completely noninvasively. There has long been interest in using this focal energy delivery to block nerve conduction for pain control and local anesthesia. In this study, we have performed an *in vitro* study to further extend our knowledge of this potential clinical application. The sciatic nerves from the bullfrog (*Rana catesbeiana)* were subjected to focused ultrasound (at frequencies of 0.661MHz and 1.986MHz) and to heated Ringer's solution. The nerve action potential was shown to decrease in the experiments and correlated with temperature elevation measured in the nerve. The action potential recovered either completely, partially or not at all, depending on the parameters of the ultrasound exposure. The reduction of the baseline nerve temperature by circulating cooling fluid through the sonication chamber did not prevent the collapse of the nerve action potential; but higher power was required to induce the same endpoint as without cooling. These results indicate that a thermal mechanism of focused ultrasound can be used to block nerve conduction, either temporarily or permanently. (E-mail: khynynen@sri.utoronto.ca) © **2009 World Federation for Ultrasound in Medicine & Biology.**

Key Words: **Ultrasound, Focused ultrasound, Therapeutic ultrasound, Nerve, Thermal damage, Bioeffects, HIFU, Ultrasound surgery.**

INTRODUCTION

The impact of ultrasound exposures on nerves has become more interesting recently with the development of a focused ultrasound phased array system that can deliver ultrasound energy through the skull under magnetic resonance imaging (MRI) guidance (Hynynen et al. 2004). Ultrasound-inhibited nerve conduction for pain management and treatment of spasticity has been actively investigated for nearly 50 years (Ballantine et al. 1960), (Foley et al. 2004, 2007, 2008). It was also recognized that focal and temporary nerve conduction inhibition could have value in investigating the central nervous system functions (Fry et al. 1958a). Although there is evidence of reversible stimulation at low ultrasound power levels (Gavrilov et al. 1996; Currier et al. 1978), the main effect that is extensively studied is the suppression of transmission along peripheral nerves and neural pathways in the brain *in vivo* (Fry et al. 1958a; Young and Henneman 1961) and in brain slices *in vitro* (Bachtold et al. 1998). However, the exact mechanism of the inhibition or the required ultrasound exposure is not clear.

To evaluate the mechanism and provide practical guidelines for further studies, we selected to conduct experiments in a simple *in vitro* frog nerve model. In prior studies it has been demonstrated that the conduction can be temporarily blocked in isolated nerves by focused ultrasound. First, Young and Henneman (1961) studied isolated frog nerves and demonstrated reversible and irreversible block in nerves that were placed in a groove made of a sound absorbing rubber. They used 2.7 MHz in 0.14–1.2 s bursts repeated at an interval of 2–3 s. In surgically-exposed cat spinal cord, reversible effects (increase or decrease) of reflexes were also induced by 3–300 bursts (duration 50–300 ms, frequency 2.7 MHz) of sonication that were repeated every 0.5–3 s (Shealy and Henneman 1962;Young and Henneman 1961). In the latter experiment, the nerve was covered by 8 or 16 mm of ultrasound absorbing mineral oil and histology

Address correspondence to: Kullervo Hynynen, Sunnybrook Health Sciences Centre, Imaging Research, and Department of Medical Biophysics, University of Toronto, 2075 Bayview Avenue, Toronto, ON, Canada, M4N 3M5. E-mail: khynynen@sri.utoronto.ca

studies showed no tissue damage in many of the experiments where the reversible effects were recorded.

The mechanisms behind the nerve conductance blocks have been attributed to ultrasound-induced temperature elevation (Lele 1963), with no evidence of any mechanical effect of ultrasound (Halle et al. 1981; Moore et al. 2000). Lele used short bursts (0.2–2 s) of ultrasound (2.7 MHz, 0.9 MHz and 0.6 MHz) at 1 s intervals until the conduction block was achieved, with most of the effects occurring at 2.7 MHz. These results explain earlier published observations (Shealy and Henneman 1962;Young and Henneman 1961); the temperature of the rubber absorber or mineral oil increased due to ultrasound absorption. These studies also found differential blocking of nerve conduction. The smallest, unmyelinated (C) fibers are the most sensitive to ultrasound. This is consistent with the clinical findings in multiple sclerosis patients, in whom conductivity of demyelinated fibers is temperature dependent. Higher temperatures worsen symptoms, while lower temperatures (as with a cold bath) usually improve the neurologic functions (Brenneis et al. 1979; Wang et al. 1999).

Focused ultrasound (FUS) can produce similar effects in the brain (in particular, the optic nerve) as seen in peripheral nerves (Fokin et al. 1979; Adrianov et al. 1984a, 1984b, 1984c, 1984d, Vykhodtseva et al. 1976). Suppression of the visual evoked potential (VEP) in both the optic nerve and visual cortex was obtained by sonications of the optic nerve in the area of its junction with the lateral geniculate nucleus. The suppression was partial or total and an increase in the amplitude (enhancement) of the VEP in the visual cortex often preceded its suppression. The extent of inhibition and degree of recovery were dependent on the ultrasound dosage. Complete recovery of all phases of the VEP usually occurred within 4–5 min but in some cases, it took 30–40 min.

A permanent nerve block model has been recently created by thermally coagulating a rabbit sciatic nerve *in vivo* (Foley et al. 2004). A 3.2 MHz FUS transducer (focal intensity between 1.5–18 kW/cm^2) was used with 30 s of sonication. Persistence of the block occurred with repeated, 5 s sonications at the intensity of 1.9 kW/cm^2 (Foley et al. 2007). Thus, mammalian nerves can be permanently blocked by sonication.

Although the previous experiments were extensive, the studies leave three questions relevant to MRI monitored transcranial ultrasound exposures. First, can the nerve block be induced with frequencies that can propagate through the skull (0.5–0.8 MHz) and is the mechanism still purely thermal at these frequencies? Second, the Lele (1963) study used multiple short bursts that induced fast temperature fluctuations. Can longer, 10–30 s continuous wave sonications that induce gradual temperature elevation that can be quantified by MRI thermometry(Hynynen et al. 2004) induce the nerve block or are high intensity bursts needed? Finally, it would be important to know if the heating of the nerve without heating the surrounding fluid could induce the same effect or is energy deposition in the surrounding tissue required. This is important since temperature gradients that may result from ultrasound absorption difference between the nerve and the surrounding fluid (or tissue) may influence the action potential. This last question is triggered by the findings of Lele (1963) who found that exposures in degassed saline (that has low ultrasound absorption and thus minimal temperature increase) were not able to induce a conduction block. The purpose of the present study is to answer these questions as a first step toward trans-skull or spinal cord MRI-guided focal inhibition of nerve conduction. In addition, *in vivo* experiments are needed to establish the temperature threshold for inducing the nerve blocks prior to the clinical feasibility of the method can be determined.

MATERIALS AND METHODS

Frog nerve dissection

All animal procedures were approved by the Harvard Animal Care Committee. Thirty, 12–15 cm long bullfrogs (*Rana catesbeiana*) were anesthetized and pithed. All frog sciatic nerves (total of 60) (diameter approximately 1–1.5 mm) were dissected from the spinal emergence to the knee and stored in normal frog Ringer's solution [110 mM NaCl, 2.5 mM KCl, 2.0 mM $CaCl_2$, 5.0 mM (N-[2-Hydroxyethyl] piperazine-N'-[2-ethanesulfonic acid]) HEPES buffer, adjusted to a pH 7.2 using 1 M NaOH].

Experimental set-up

The nerve stimulation holder (8 × 4.5 × 2.5 cm) was acrylic and contained three chambers. The end chambers were 2 × 2 × 1.3 cm and the center holder contained a 2.4 cm diameter hole fitted with a coil of 3.2 mm copper tubing around the circumference for heating and cooling of the sonication chamber. The three chambers were separated by 3 mm thick partitions with a 2 mm wide by 8 mm deep groove for the placement of the nerve. A 0.04 mm thick mylar sheet was glued to the groove bottom to create an access point for the ultrasound beam to target the nerve. A thermocouple was mounted in the sonication chamber to measure the fluid temperature. All of the chambers were filled with frog Ringer's solution and the nerve placed in the chamber such that it had good electrical contact with the measuring and stimulating electrodes. Following the nerve positioning in the holder, the end-stimulating and recording pools were evacuated of Ringer's solution and replaced by mineral oil to assure electrical isolation. The Ringer's solution temperature

was monitored and maintained at room temperature (approximately 20–23 °C) unless otherwise stated.

Nerve stimulation and recording was accomplished using a routine set-up (Fig. 1): a stimulator (model S48; Grass Technologies, West Warwick, RI, USA), stimulus isolation unit (Model SIU5; Grass Technologies) was attached to the bipolar electrodes in one end well and a stimulus applied at 50 μs duration, with intensity set at ~1.25 times that which gave the maximum height of the compound action potential (CAP). The other end pool contained the recording bipolar electrodes, which were connected to an AC amplifier (Model CP511; Grass Technologies) and the amplified compound action potentials were viewed on a oscilloscope (Model TDS 3012; Tektronix Inc., Richardson, TX, USA). The recorded CAP is the result of simultaneous excitation of all of the ~1000 large myelinated axons in this nerve. Each individual fiber would have, on average a ''unit action potential'' that is 0.001–0.002 of the amplitude of the CAP and a duration at half-height of ~0.25 that of the CAP; the broader CAP signal results from the dispersion of the unit APs that have a range of conduction velocities and so arrive at the recording electrodes at different times.

An FUS beam was generated with a wave form generator (Wavetek Model 395; San Diego, CA, USA), radio-frequency (RF) power amplifier (Model 2100L; ENI, Rochester, NY, USA) and an in-house constructed, spherically-curved transducer (diameter 10 cm, radius of curvature 8 cm) with the fundamental frequency of 0.661 MHz (FL) and the third harmonic frequency of 1.986 MHz (FH). The transducer was matched to the power output of the amplifier by external LC-circuits at these frequencies. The applied RF-power was measured using a power meter (HP 438A; Hewlett Packard, Palo Alto, CA, USA) and dual directional coupler (Werlatone model C2625; Verlatone Inc., Brewster, NY, USA). The acoustic power was measured as a function of the applied RF-power using a radiation force method (Hill 1970). This method is absolute and has been verified against a calorimeter method (Hynynen 1993). The peak pressure amplitude was measured using a PVDF, coplanar-shielded membrane hydrophone (GEC-Marconi Research Center, Chelmsford, England) with an active area of 0.5 mm in diameter. The hydrophone was calibrated by the National Physics Laboratory, Teddington, Middlesex, England. This calibration was done at the low pressure amplitudes and then extended to the higher pressures, based on the total, measured acoustic power. This extrapolated pressure amplitude was used to calculate the spatial peak, temporal peak intensity at the focus. The measured half-maximum beam diameter was approximately 2.2 mm and 0.8 mm for the FL and FH, respectively.

The ultrasound transducer was mounted in an acrylic container (28 cm × 24 cm × 14 cm high.) An adjustable plate with a mylar window was used to hold the measurement chamber with the mounted nerve, allowing the nerve to be moved in three dimensions in order to focus the ultrasound beam on the nerve. A cylindrical, water-filled acrylic tube was placed on top of the nerve, such that the ultrasound beam could propagate into the water column. At the top end of the chamber, a rubber absorber was used to eliminate ultrasound reflections. Figure 1 shows the layout of experimental set-up.

Sonication and temperature measurements

The sonications were mostly continuous wave exposures, except for 26 experiments in which five nerves were exposed to burst sonication to determine the feasibility of reducing the time-average power and the temperature elevation. These sonications had a burst length of 1 and 10 ms, with a repetition frequency of 10 and 20 Hz. In addition, one nerve group received heated Ringer's (HR) solution in place of ultrasound. Groups receiving sonication were given a 30 s exposure, followed by a 60 s ''off'' period followed, by a new sonication at an increased acoustic power. This was repeated until the elimination

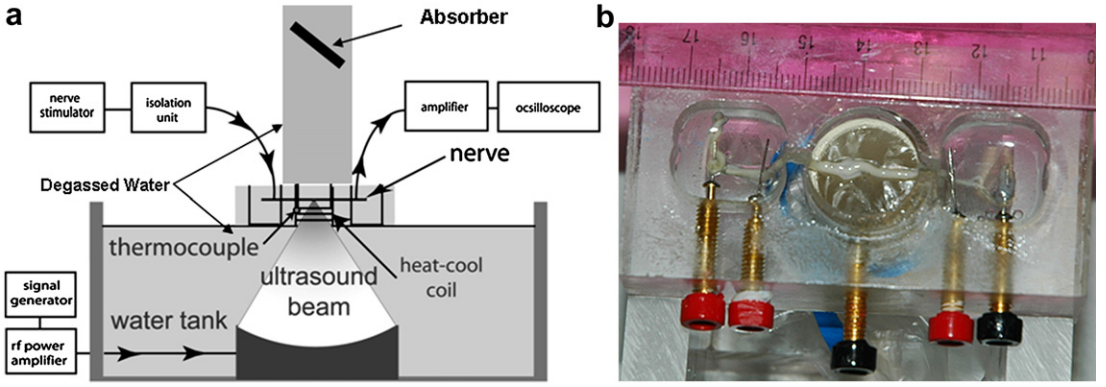

Fig. 1. Experimental set-up. (a) Schematic vertical cross section of the sonication set-up. (b) Photograph of the nerve chamber, from above, showing the nerve mounted on stimulating and recording electrodes in the lateral pools.

of action potential was seen or the maximum power was reached. The experiments were repeated if the action potential recovered. Two nerves receiving continuous sonications (FH, FL) and the heated Ringer's solution (HR) nerve had a thermocouple placed inside each nerve to measure the intra-nerve temperature. A thermocouple (copper-constantan, wire diameter 50 μm, bare junction), with the aid of a lead wire, was attached to a needle and then put into the nerve. The beam focus was aimed to get the maximum temperature in the thermocouple. Based on heat transfer the centre of the nerve (thermocouple location) should have the highest temperature. The viscous heating artifact (Fry and Fry 1954) was estimated using the temperature decay method after the power was turned off (Parker 1983). For the HR group, heated water circulating through the copper coil in the sonication pool raised the temperature of the Ringer's solution around the nerve. The heating rate varied between 0.022 and 0.007 °C/s for these experiments.

Histology

For histologic evaluation, six segments of the nerves were fixed in 10% formalin at room temperature, embedded in paraffin, cut longitudinally and impregnated with silver or stained with hematoxylin and eosin (H&E). The histologist was blinded towards the sonication parameters.

RESULTS

Measurements

Figure 2 shows a 30 s sonication at 16 W (average power during the burst) that produced a temporary loss of action potential. The spatial peak, temporal average intensity during the 30 s continuous wave sonication was approximately 440 W/cm^2 that resulted in a temperature of approximately 33 °C in a similar nerve in a separate experiment. The compound action potential decreased during the sonication and was almost completely eliminated at 3 min post-sonication. There was also a shortened latency between the stimulus artifact and the action potential rise and peak 1 min post-sonication. At higher power levels than 16 W (= 440 W/cm^2), the signal was totally abolished during the sonication in this experiment.

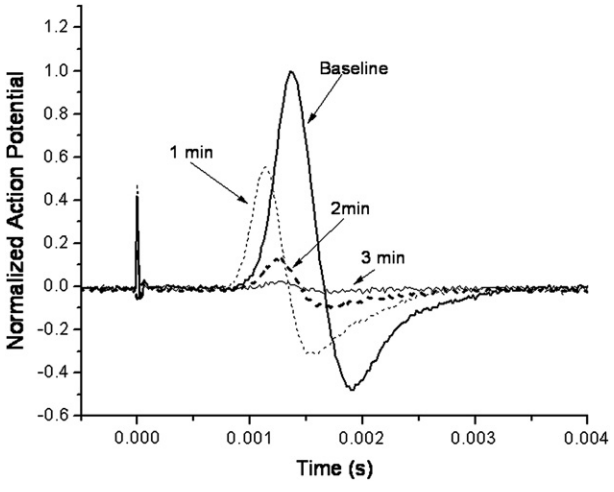

Fig. 2. An example of the reduction of the action potential after a 30 s sonication at the frequency of 0.661 MHz and at the acoustic power of 16 W. The ringer solution temperature was maintained at room temperature (20–23 °C).

Figure 3 plots the mean value and the standard deviation of the smallest, normalized action potential attained as a function of the peak intensity (spatial peak, temporal average intensity during the 30 s continuous wave sonication) at the focus, for both of the frequencies used. A detectable reduction in the action potential was induced with both frequencies at an intensity of approximately 100–200 W/cm^2, with reducing signal as a function of increasing intensity. For both frequencies, the action potential amplitude was halved at 300–350 W/cm^2. There was a residual action potential up to 575 and 875 W/cm^2 at the low and high frequency, respectively.

The action potential recovered differently in the tested nerves after the initial sonication. Figure 4 shows an example of the observed action potential recovery as

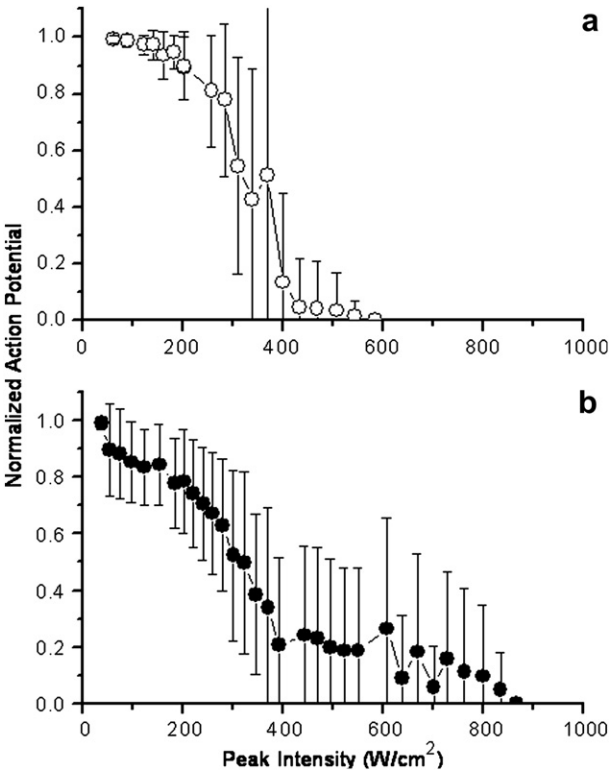

Fig. 3. Mean action potential change of the nerves exposed to ultrasound as a function of the focal peak intensity at the frequency of 0.661 (a) and 1.981 MHz (b) The Ringer's solution temperature was maintained at room temperature (20–23 °C).

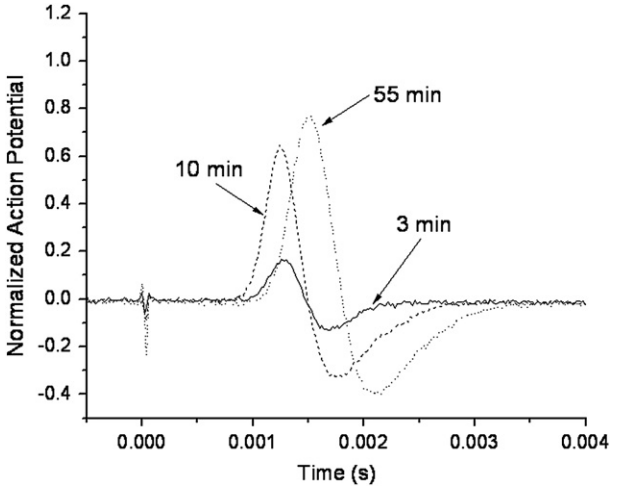

Fig. 4. Recovery of action potential after a complete conduction block induced by a 30 s sonication at the frequency of 0.661 MHz at the acoustic power of 16 W. The Ringer's solution temperature was maintained at room temperature (20–23 °C).

a function of time after sonication (same sonication parameters as in Fig. 2) and Figure 5 graphs a recovery of three different nerves sonicated at 0.661 MHz for 30 s. One of the nerves (sonicated at 370 W/cm^2) recovered completely, in approximately 90 min, another (sonicated at 400 W/cm^2) showed only partial recovery of the action potential and in the third nerve (sonicated at 650 W/cm^2), the action potential was completely and permanently eliminated. This happened at the highest exposure levels with average intensity of 470 and 418 W/cm^2 at the LF and HF, respectively. In some cases these nerves showed macroscopic damage. In 60% of the nerves that initially completely lost action potential (sonicated at or above 370 W/cm^2), then recovered it, the action potential was detected within the first minute. One hundred percent of the nerves showed a signal at 4 min following the complete loss of the action potential (Fig. 6).

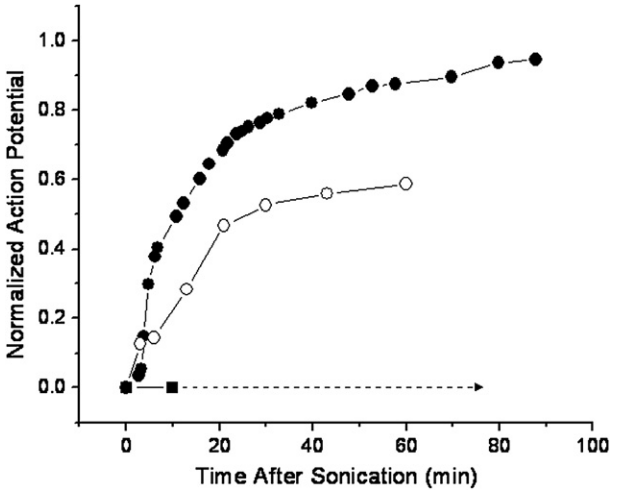

Fig. 5. Normalized action potential recovery after a complete conduction block as a function of time after the 30 s sonications at the frequency of 0.661 MHz . One of the nerves (sonicated at approximately 370 W/cm^2) recovered completely, in approximately 90 min, another (sonicated at approximately 400 W/cm^2) showed only partial recovery of the action potential, and in the third nerve (sonicated at approximately 650 W/cm^2), the action potential was completely and permanently eliminated. The Ringer's solution temperature was maintained at room temperature (20–23 °C).

The temperature elevation reached steady-state after approximately 12 s sonication. When nerve action potential was plotted as a function of this peak temperature, it was found to decrease with increasing temperature. Action potentials reached zero at approximately 37 °C for the low frequency exposures and at 43 °C for high frequency exposures (Fig. 7). The nerves that were heated with water followed the pattern of the higher frequency exposures.

When the temperature of the Ringer's solution was reduced to 9 °C, the action potential (as a function of peak intensity) decreased proportionally, up to approximately 50% reduction from its initial value, after which the colder fluid protected the nerve for the low frequency exposure. For the high frequency, the protection was observed throughout the intensity range (Fig. 8).

The action potential as a function of the intra-nerve temperature was plotted (Fig. 9) for the burst sonications with the burst length of 10 ms and repetition frequency of 10 or 20 Hz. The temperature elevation was limited by the low duty cycle and only a small decrease in the action potential was detected. The action potential was

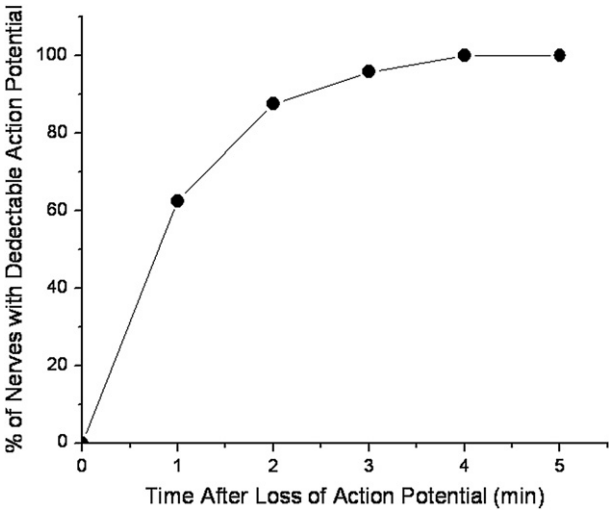

Fig. 6. Cumulative percentage of nerves having detectable action potential after sonication that induced a complete conduction block. Only the nerves that recovered completely were included in this graph. The nerves were sonicated for 30 s at or above 370 W/cm^2 with the frequency of 0.668 MHz. The Ringer's solution temperature was maintained at room temperature (20–23 °C).

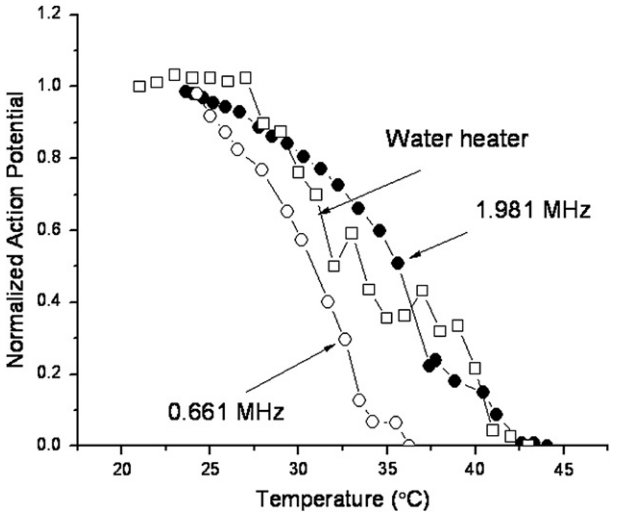

Fig. 7. Action potential as a function of nerve temperature for the sonicated and water bath heated nerves (one nerve each). A similar result was observed in a repeat experiment with different nerves.

observed to decrease with increasing temperature except for the case of HF burst at the PRF of 10 Hz that showed a small (approximately 2%–3%) increase.

Histologic findings

We stained and examined the nerves that had complete conduction block after several sonications. In longitudinal sections stained with H&E or impregnated with silver, three patterns appeared: (1) the specimen was indistinguishable from an unexposed nerve; (2) the exposed nerve was mostly intact but contained small areas that showed disorganization in the nerve structure; and (3) the nerve was irreversibly damaged. Overall, the histology demonstrated minimum damage at the higher frequency and severe damage at the lower frequency sonications.

Pattern 1. Examples of the histology for the low frequency, 0.661 MHz sonications where the conduction was completely blocked are shown in Figure 10. H&E-stained, undamaged nerves maintained parallel nerve fibers as well as normal Schwann cell outlines and nuclei (Fig. 10B and shown by arrows in Fig. 10C). In the silver-stained sections, the axons appear as dark, dense structures, separated with large, clear spaces.

Pattern 2. In some cases, the distribution of the changes within treated segments was nonuniform. The majority of a segment would appear microscopically identical to the untreated nerve, however, one part of this segment would contain one to three small regions in which the nerve structure appeared to be disorganized (Fig. 10F). In these areas, some myelin sheaths were fragmented into globules (Fig. 10 G) and nuclei of the Schwann cells were pyknotic. Although the axis cylinders appeared to be

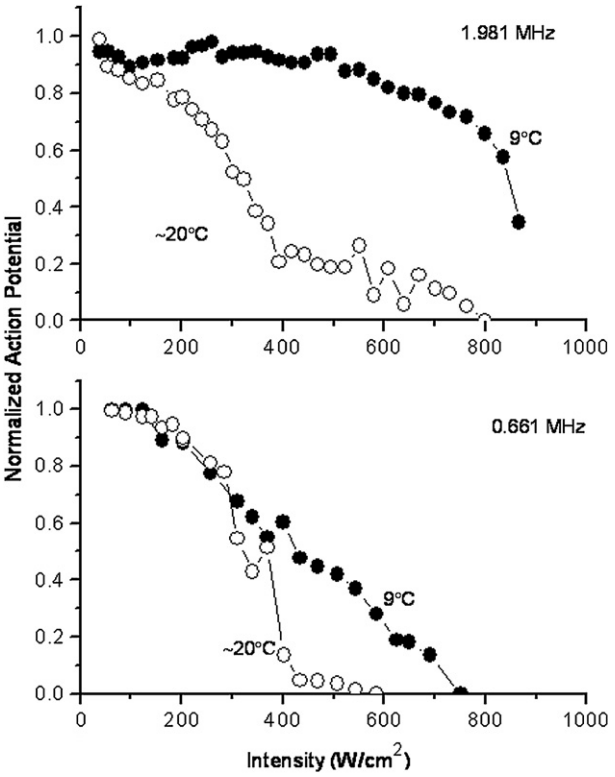

Fig. 8. Normalized action potential as a function of the peak intensity for the two surrounding liquid temperatures for both frequencies (0.661 and 1.981 MHz).

continuous and normal, a few seemed to be slightly swollen and uneven (Fig. 10H).

Pattern 3. In the case of irreversible damage, the treated segments were swollen and torn apart

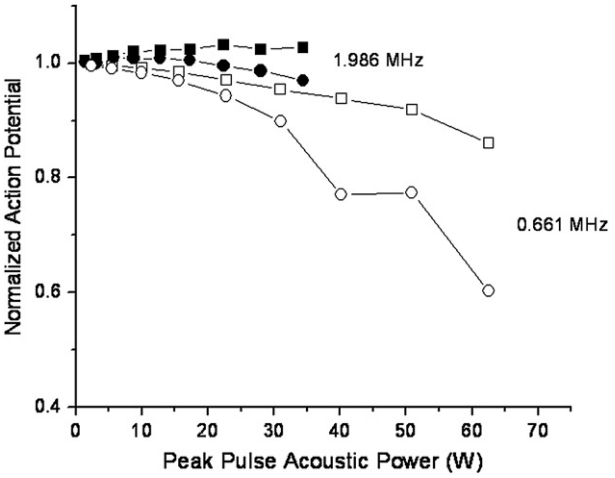

Fig. 9. Normalized action potential as a function of the measured nerve temperature for the burst sonications. The burst length was 10 ms and the pulse repetition frequency was 10 or 20 Hz and the total sonication duration 30 s. The open and closed symbols are for the frequencies of 0.661 and 1.986 MHz, respectively.

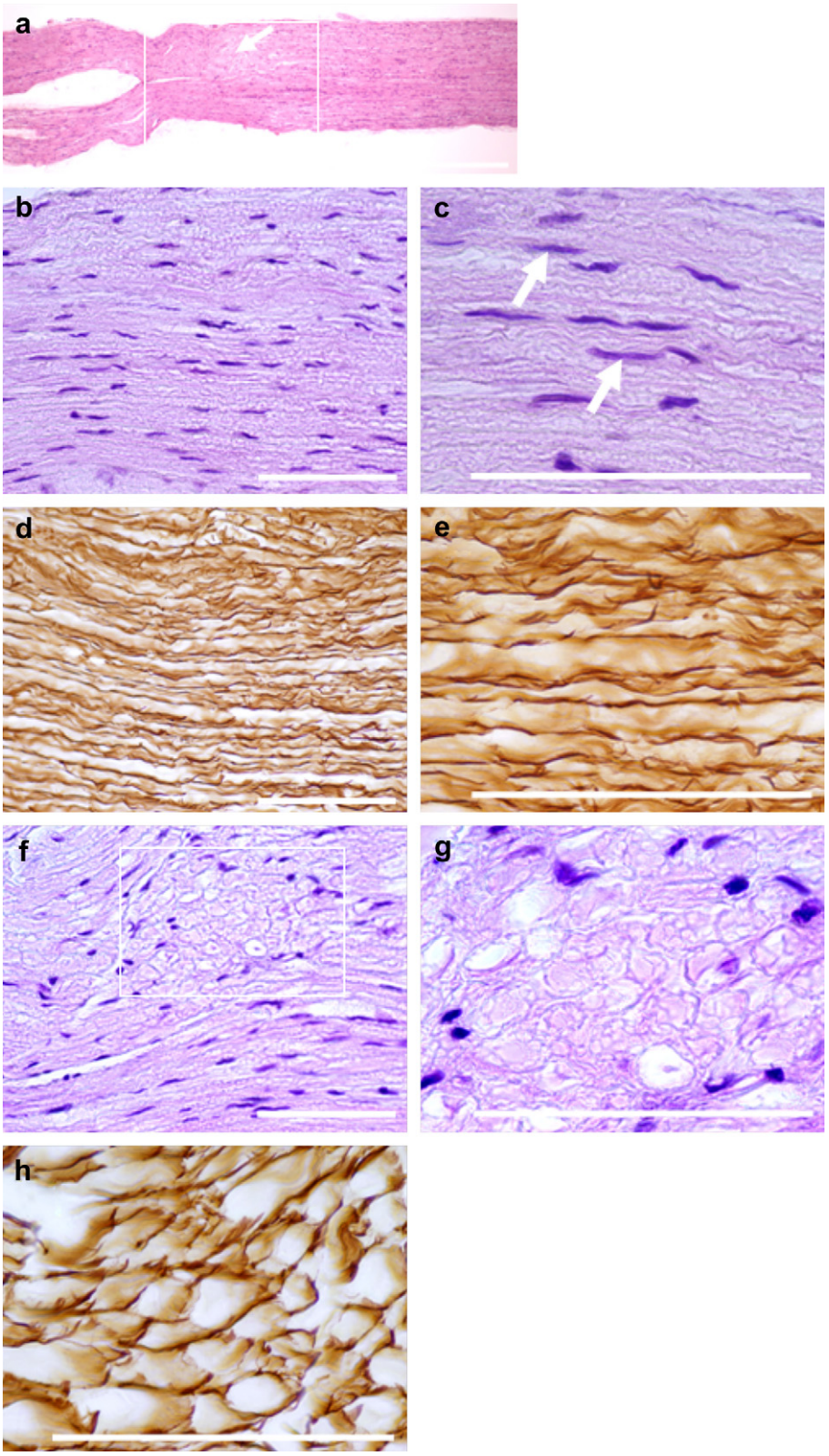

Fig. 10. Microphotographs (pattern 2, described in the results) of the longitudinal sections of the frog sciatic nerve treated with focused ultrasound (FUS): (a) Low magnification of the nerve; the treated segment is shown in the boxed area; (b)–(e) Untreated nerve segment demonstrates parallel nerve fibers and normal Schwann cell nuclei (arrows in c); (f)–(h) Small area (arrow in a), in which the nerve structure is disorganized; with some myelin sheaths are fragmented into globules (g) and Schwann cell nuclei appear pyknotic; axis cylinders are mostly undamaged (h). Staining: (a), (b), (c), (f), (g) = H&E; (d), (e), (h) = silver impregnation. Bars: (a) = 1 mm; (b)–(h) = 100 μm.

(Fig. 11A). Myelin sheaths were profoundly affected: most myelin sheaths were fragmented into globules. The axis cylinders had a nodular appearance or were fragmented into swollen vacuolated globules. Many axis cylinders developed ovoid and spherical forms, which were connected by thin threads, like pearls on strings (Fig. 11B and C). In some areas, the fibers were completely dissociated into free spheres (Fig. 11D and E). The myelin sheaths were very pale and frequently, barely visible at all (Fig. 11F).

The higher frequency sonications showed either no evidence of tissue damage or minor damage (similar to Fig. 10) after multiple sonications (data not shown).

DISCUSSION

FUS exposures of an *in vitro* frog nerve can temporarily or permanently block nerve conduction. A temporary block resulted in the action potential returning within 4 min but full recovery of the action potential took up to 90 min. At higher power levels and repeated exposures, the action potential could be completely eliminated. At the higher frequency (nearly 2 MHz), nerve conduction block was similar to that induced by elevated temperature alone. This supports the previous observation of the role of temperature in blocking the nerve conduction in studies where nerve surroundings were the major energy absorbers (Lele 1963;Young and Henneman 1961). Histology of these nerves demonstrated little or no damage, indicating that with appropriate monitoring of the thermal exposure, a transient and repeatable nerve block can be induced.

At high sonication frequencies (almost 2 MHz), nerve temperature elevation was an adequate explanation of our observations. We indirectly verified a thermal mechanism underlying FUS nerve blockade since water bath heating of the nerve resulted in a similar temperature vs. action potential curve and cooling of the nerve increased the power requirements. Our results are consistent with published observations (Lele 1963) showing that 2.7 MHz and 0.9 MHz burst sonications of a nerve in absorbing fluid caused a conduction block identical to a thermally-induced block at temperatures between 41 and 45 °C. Although transient auditory nerve block has also been demonstrated during fever in three children (Starr et al. 1998), the exact mechanism how temperature elevation causes the reversible inhibition of the action potential is not completely understood. It has been proposed that temperature-induced changes in the kinetics of ion channels can explain the transient temperature induced conduction block. Xu and Pollock (1994) explained that the rise in temperature both increases the rate of activation and inactivation of the sodium channels. Since the impact on the inactivation is larger the temperature increase eventually resulting in Na+ inactivation and K+ activation encroach on Na+ activation time. This causes the repolarization to occur before there is sufficient sodium current to generate a propagating pulse. This could explain the delay seen in the reduction of action potential after the sonication (Fig. 2).

At the lower frequency of 0.661 MHz (a frequency suitable for trans-skull sonications), the action potential reduction was reached at approximately 5 °C lower temperatures, indicating additional, nonthermal mechanisms may be in play. The cooling of the nerve to 9 °C did not change the required intensity at the lower frequency but protected the nerve from losing the action potential completely at the higher frequency. This supports the observation that there must also be a nonthermal mechanism *in vitro* nerve inhibition. In fact, an *in vitro* brain slice study (Bachtold et al. 1998) that used 500 kHz bursts, repeated at the frequency of 200 kHz, found an approximately 30% depression of nerve signaling that was only partially explained by temperature elevation. Perhaps the large (0.25 mm in diameter) thermocouple probe used in that study may have recorded lower than actual tissue temperature due to thermal conduction along the probe in the steep thermal gradients present in the experimental setting (Samulski et al. 1985).

In our experiments, the mechanism of the nonthermal effect was not clear. Histology observations indicated mechanical damage to part of some of the nerves exposed at 0.661 MHz. Thus, limited cavitation caused by trapped microbubbles may have been responsible for this added effect, either by increasing the local microscopic temperature (and increasing the local radiation-force-mediated mechanical force on the nerve) or inducing direct mechanical damage by shock waves caused by the collapsing bubbles. Although we tried to avoid the possibility of cavitation in the surrounding fluid by carefully degassing the Ringer's solution, there may have been enough gas to permit cavitation at the high intensities used in these experiments. Therefore, we would expect that the lower frequency would produce only thermal effects *in vivo*, where the gas bubbles are not present since the sonication intensities would likely be below the inertial cavitation threshold in brain (Vykhodtseva et al. 1995).

The burst sonications produced a small initial increase and then reduction in the action potential that was proportional to the reduced time average power and induced temperature elevation. These results differ from a published one (Mihran et al. 1990) that demonstrated modification of the electrical excitability (enhancement and depression) of frog sciatic nerve by FUS bursts of 0.5 ms, at the intensity of 100–800 W/cm^2 over frequencies of 2–7 MHz without significant temperature

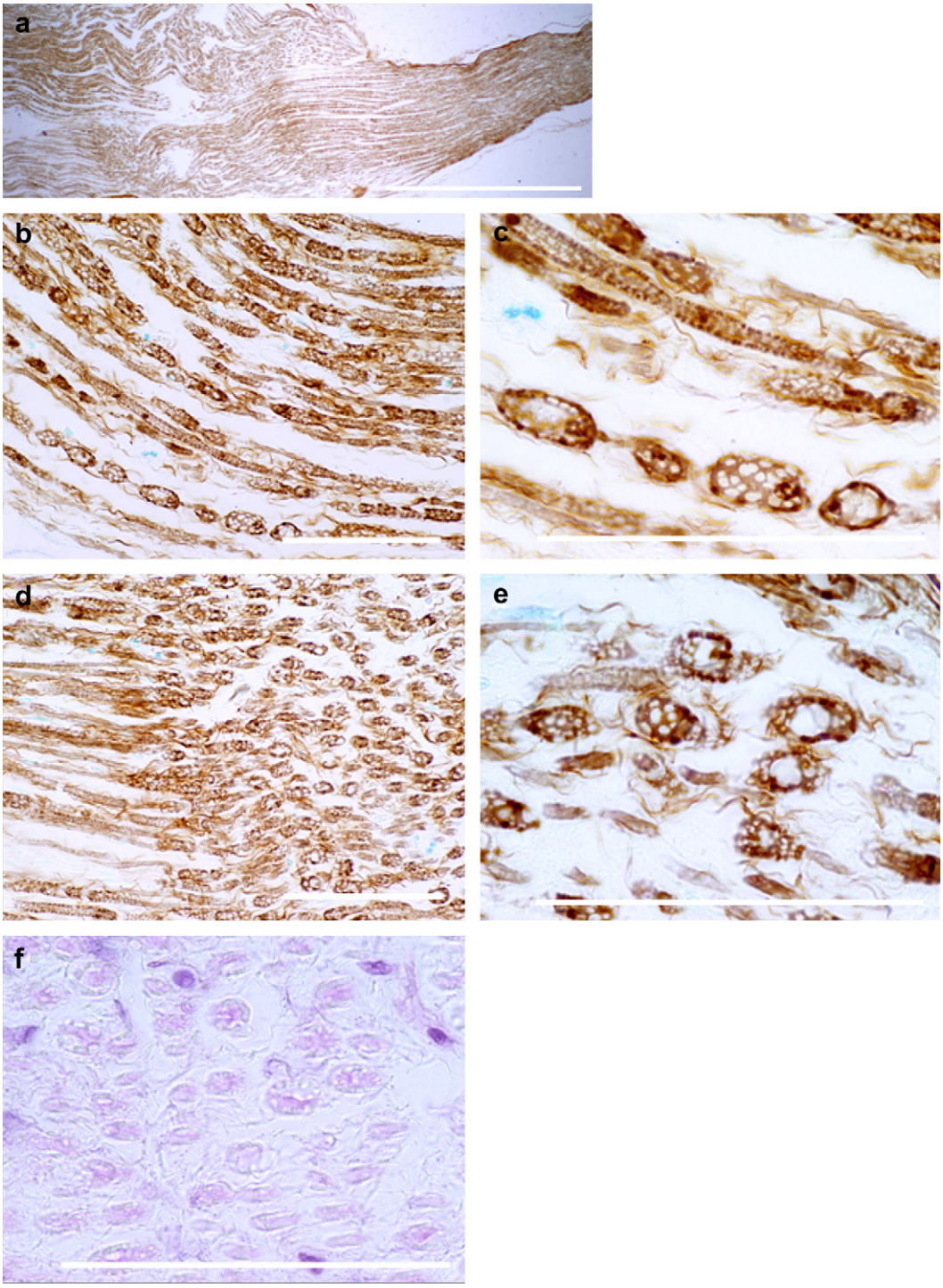

Fig. 11. Microphotographs (pattern 3, described in the results) of the longitudinal sections of the frog sciatic nerve treated with focused ultrasound (FUS): (a) The low magnification irreversibly damaged nerve; the treated nerve segment appears swollen and torn apart; (b)–(c) The degenerated axis cylinders are swollen and vacuolated. Many of them develop ovoid and spherical forms assuming the appearance of a string of beads; (d)–(f) Some fibers are completely dissociated into free spheres; (f) The myelin sheaths are fragmented into pale barely visible globules. Bars: (a) = 1 mm; (b)–(f) = 100 μm. Staining: (a)-(e) = silver impregnation; (f) = H&E.

elevation. These authors suggested that an activation of stretch-sensitive ionic channels (through conformational changes due to membrane tension) by the radiation pressure was responsible for these effects. Importantly, these authors did not use degassed fluid around the nerve, thus, cavitation in the liquid may explain at least part of

the deviation from our results. This explanation is partially supported by a shock wave study (pressure amplitudes up to over 100 MPa, duration of $\sim$ 2 μs) that induced compound action potentials similar to those generated by electrical stimulation in frog sciatic nerve (Schelling et al. 1994). Bioeffects of shock waves on nerves were induced mostly when gas bubbles were present in the surrounding fluid.

Gavrilov et al. (1996) reviewed studies investigating the feasibility of the use of focused ultrasound for stimulation of the superficial and deep-seated receptor structures of humans and animals. They proposed that the main effect of focused ultrasound in stimulating neural structures is mechanical force that could produce a change in membrane potential resulting in the stimulation of neural structures.

One limitation of our *in vitro* experiments is that the nerve is comprised of many fibers that collectively contribute to the action potential signal. The compound action potential arises from the large myelinated axons but pain is conducted by small myelinated and nonmyelinated axons. Based on the work of Young and Henneman (1961), peripheral nerves have fibers with different conduction velocities, due to the degree of myelination. According to their study, the unmyelinated C fibers are the most sensitive to ultrasound and heat and Alpha fibers with the thickest myelin sheath are the least sensitive. In our experiments, the ultrasound intensity across the whole bundle was relatively constant, especially at the lower frequency, however, the induced temperature elevation had large gradients such that the central parts were warmer due to the thermal energy loss by free fluid convection around the nerve. Another limitation in the current experiments is that the nerves used come from a cold-blooded amphibian. Therefore, the impact of sonications on the nerves of humans whose temperature is very tightly controlled may not be exactly the same as shown by our results. Thus, *in vivo* experiments are needed to fully explore the utility of the thermal effects of sonications for inducing conduction block.

The first obvious application of FUS induced permanent nerve block is for pain treatment. Ultrasound irradiation has been used to treat neuroma, painful amputation stump neuromas and phantom limbs (Chateau 1951; Young and Henneman 1961) (Tepperberg and Marjey 1953). Transcutaneous FUS (2.7 MHz; 1–3 min; 1700 W/cm^2; 0.14 s burst; 3 s pulse period; three sets of three pulses each, with each set separated by an interval of 1 min) has been used on seven patients with painful neuromas. Sonication of peripheral nerves 1 to 3 mm proximal to the neuroma resulted in complete relief of pain without loss of sensation in 7 of 10 neuromas and, in three cases, partial relief was achieved. With careful control of the induced temperature, even better clinical results should be achieved. While sonication of sensory fibers results in pain management, similar conduction blockage of motor nerves can be used to alleviate the symptoms of spasticity (Ballantine et al. 1960; Foley et al. 2004, 2007, 2008).

MRI-guided FUS could also be clinically applied to inhibit brain function by causing conduction blockage of the fibers or fiber tracts of the white matter, or by inhibiting the function of neurons at the cortex or at subcortical nuclei. With MRI-guided FUS (Hynynen et al. 2004), nerve conductance blockage can be performed at desired locations of the brain to study function or even treat disorders. FUS can be used like another noninvasive method, transcranial magnetic stimulation (TMS), for both diagnosis and therapy (Kluger and Triggs 2007;Hallett 2007). FUS is advantageous over TMS for a variety of reasons. FUS gives better localization and targeting (the focus area is much smaller than the effective volume of TMS and FUS focus can be localized with temperature sensitive imaging on MRI (Hynynen et al. 1997)). While TMS can be used in deep brain tissues, FUS can penetrate all the way into the central structures of the brain while maintaining highly focused energy delivery. Pioneering studies (Fry 1958) of FUS-produced, reversible functional changes deep within the lateral geniculate nucleus (site of synaptic relay point along the visual pathway), provided reversible interruption of information transfer along a neural pathway. These researchers were also first to suggest using FUS-induced reversible changes for the three-dimensional functional mapping of the central nervous system (Fry et al. 1958b). Their suggestion is applicable with current technology, where trans-skull exposures of ultrasound can be delivered under MRI guidance with careful online temperature control. MRI can also be used to map the function in the brain such that desired functional targets or disorders can be precisely exposed.

In conclusion, our study has further investigated the feasibility of using FUS to temporarily block nerve conduction in frog nerves *in vitro*. We verified earlier observations that temperature elevation is the main reason for the induced block and that function will recover within minutes after the exposure if the block is reversible. We also demonstrated that a frequency (0.661 MHz) suitable for trans-skull sonication can induce a reversible block at reduced, macroscopic temperature elevation. This reduction in the required temperature elevation was at least partially attributed to cavitation present in the experimental system. Further studies are required to investigate if a similar gain can be induced *in vivo*.

Acknowledgements—This research was partially supported by a gift from Haim Saban, Maurice Kanbar and Brainsonix Corp, and by National Institutes of Health grant U41RR019703.

REFERENCES

Adrianov OS, Vykhodtseva N, Fokin VF, Avirom VM. Method of local action by focused ultrasound on deep brain structures in unrestrained unanesthetized animals. Biull Eksp Biol Med 1984a;98:115–117.

Adrianov OS, Vykhodtseva N, Fokin VF, Uranova N, Avirom VM. Reversible functional shutdown of the optic tract on exposure to focused ultrasound. Biull Eksp Biol Med 1984b;97:760–762.

Adrianov OS, Vykhodtseva NI, Fokin VF, Avirom VM. [Method of local action by focused ultrasound on deep brain structures in unrestrained unanesthetized animals] Metod lokal'nogo vozdeistviia fokusirovannym ul'trazvukom na gluboko raspolozhennye struktury mozga neobezdvizhennogo nenarkotizirovannogo zhivotnogo. Biull Eksp Biol Med 1984c;98:115–117.

Adrianov OS, Vykhodtseva NI, Gavrilov LR. [Use of focused ultrasound for local effects on deep brain structures] Primenenie fokusirovannogo ul'trazvuka dlia lokal'nogo vozdeistviia na glubokie struktury mozga. Fiziol Zh SSSR 1984d;70:1157–1166.

Bachtold MR, Rinaldi PC, Jones JP, Reines F, Price LR. Focused ultrasound modifications of neural circuit activity in a mammalian brain. Ultrasound Med Biol 1998;24:557–565.

Ballantine HTJ, Bell E, Manlapaz J. Progress and problems in the neurological applications of focused ultrasound. J Neurosurg 1960;17: 858–876.

Brenneis M, Harrer G, Selzer H. [On the temperature sensitivity of multiple sclerosis patients (author's transl)]. Fortschr Neurol Psychiatr Grenzgeb 1979;47:320–325.

Chateau A. [Recent applications of ultrasonic therapy: phantom limb]. J Radiol Electrol Arch Electr Medicale 1951;32:513–514.

Currier DP, Greathouse D, Swift T. Sensory nerve conduction: effect of ultrasound. Arch Phys Med Rehabil 1978;59:181–185.

Fokin VF, Chepkunov AV, Avirom VM, Vykhodtseva N. Production of reversible functional changes in the visual system of the cat brain by focused irradiation of the optic nerve Puschino, Russa. Moscow, USSR: All-Union Academy of Science 1979;12-15.

Foley JL, Little JW, Starr FL III, Frantz C, Vaezy S. Image-guided HIFU neurolysis of peripheral nerves to treat spasticity and pain. Ultrasound Med Biol 2004;30:1199–1207.

Foley JL, Little JW, Vaezy S. Image-guided high-intensity focused ultrasound for conduction block of peripheral nerves. Ann Biomed Eng 2007;35:109–119.

Foley JL, Little JW, Vaezy S. Effects of high-intensity focused ultrasound on nerve conduction. Muscle Nerve 2008;37:241–250.

Fry FJ, Ades HW, Fry WJ. Production of reversible changes in the central nervous system by ultrasound. Science 1958a;127:83–84.

Fry WJ. Intense ultrasound in investigations of the central nervous system. Adv Biol Med Phys 1958;6:281–348.

Fry WJ, Fry RB. Determination of absolute sound levels and acoustic absorption coefficients by thermocouple probes- experiment. J Acoust Soc Am 1954;26:311–317.

Fry WJ, Meyers R, Fry FJ, Schultz DF, Dreyer LL, Noyes RF. Topical differentia of pathogenic mechanisms underlying Parkinsonian tremor and rigidity as indicated by ultrasonic irradiation of the human brain 1958b;16–24.

Gavrilov LR, Tsirulnikov EM, Davies IA. Application of focused ultrasound for the stimulation of neural structures. Ultrasound Med Biol 1996;22:179–192.

Halle JS, Scoville CR, Greathouse DG. Ultrasound's effect on the conduction latency of the superficial radial nerve in man. Phys Ther 1981;61:345–350.

Hallett M. Transcranial magnetic stimulation: a primer. Neuron 2007; 19(55):187–199.

Hill CR. Calibration of ultrasonic beams for biomedical applications. Phys Med Biol 1970;15:241–248.

Hynynen K. Acoustic power calibrations of cylindrical intracavitary ultrasound hyperthermia applicators. Med Phys 1993;20:129–134.

Hynynen K, Clement GT, McDannold N, *et al*. 500-element ultrasound phased array system for noninvasive focal surgery of the brain: A preliminary rabbit study with *ex vivo* human skulls. Magn Reson Med 2004;52:100–107.

Hynynen K, Vykhodtseva NI, Chung A, Sorrentino V, Colucci V, Jolesz FA. Thermal effects of focused ultrasound on the brain: Determination with MR Imaging. Radiology 1997;204:247–253.

Kluger BM, Triggs WJ. Use of transcranial magnetic stimulation to influence behavior. Curr Neurol Neurosci Rep 2007;7:491–497.

Lele PP. Effects of focused ultrasonic radiation on peripheral nerve, with observations on local heating. Exp Neurol 1963;8:47–83.

Mihran RT, Barnes FS, Wachtel H. Temporally-specific modification of myelinated axon excitability *in vitro* following a single ultrasound pulse. Ultrasound Med Biol 1990;16:297–309.

Moore JH, Gieck JH, Saliba EN, Perrin DH, Ball DW, McCue FC. The biophysical effects of ultrasound on median nerve distal latencies. Electromyogr Clin Neurophysiol 2000;40:169–180.

Parker KJ. The thermal pulse decay technique for measuring ultrasonic absorption coefficients. J Acoust Soc Am 1983;74:1356–1361.

Samulski TV, Lyons BE, Britt RH. Temperature measurements in high thermal gradients: II. Analysis of conduction effects. Int J Radiat Oncol Biol Phys 1985;11:963–971.

Schelling G, Delius M, Gschwender M, Grafe P, Gambihler S. Extracorporeal shock waves stimulate frog sciatic nerves indirectly *via* a cavitation-mediated mechanism. Biophys J 1994;66:133–140.

Shealy CN, Henneman E. Reversible effects of ultrasound on spinal reflexes. Arch Neurol 1962;6:374–386.

Starr A, Sininger Y, Winter M, Derebery MJ, Oba S, Michalewski HJ. Transient deafness due to temperature-sensitive auditory neuropathy. Ear Hear 1998;19:169–179.

Tepperberg I, Marjey Ej. Ultrasound therapy of painful postoperative neurofibromas. Am J Phys Med 1953;32:27–30.

Vykhodtseva NI, Gavrilov LR, Mering TA, Iamshchikova NG. [Use of focused ultrasound for local destruction of different brain structures] Primenenie fokusirovannogo ul'trazvuka dlia lokal'nykh razrushenii razlichnykh struktur golovnogo mozga. Zh Nevropatol Psikhiatr 1976;76:1810–1816.

Vykhodtseva NI, Hynynen K, Damianou C. Histologic effects of high intensity pulsed ultrasound exposure with subharmonic emission in rabbit brain *in vivo*. Ultrasound Med Biol 1995;21:969–979.

Wang AK, Raynor EM, Blum AS, Rutkove SB. Heat sensitivity of sensory fibers in carpal tunnel syndrome. Muscle Nerve 1999;22: 37–42.

Xu D, Pollock M. Experimental nerve thermal injury. Brain 1994;117: 375–384.

Young RR, Henneman E. Functional effects of focused ultrasound on mammalian nerves. Science 1961;134:1521–1522.